16th European Signal Processing Conference (EUSIPCO 2008), Lausanne, Switzerland, August 25-29, 2008, copyright by EURASIP

PERFORMANCE CHARACTERIZATION OF AN IMAGING SPECTROGRAPH FOR THE ACQUISITION AND ANALYSIS OF MULTISPECTRAL IMAGES

Anna Paviotti[1] *and Luca Poletto*[2]

[1] LTTM Laboratory
Department of Information Engineering
University of Padova (Italy)
via Gradenigo 6/B, 35131, Padova, Italy
lttm.dei.unipd.it
{paviotti,brusco}@dei.unipd.it

[2]LUXOR Laboratory
CNR - Istituto Nazionale per la Fisica della Materia
c/o Department of Information Engineering
University of Padova (Italy)
www.dei.unipd.it\luxor
poletto@dei.unipd.it

ABSTRACT

This paper presents a performance characterization of the Specim ImSpector V10[1] used as the core of a spectral camera for the acquisition and analysis of works of art. The Specim ImSpector is an imaging spectrograph generally used for colorimetry applications. Our purpose is to employ it for the analysis of the spectral content in the visible and near infrared spectrum of a fragment of the mosaic of St.Mark's Basilica in Venice (Italy). After spectral calibration, we assessed the system performance by acquiring a set of calibrated tiles under different illumination sources. The best results were obtained by combining the spectral reflectances measured with a lithium lamp and with a common incandescence bulb.

1. INTRODUCTION

Multispectral imaging has been gaining increasing importance in the cultural heritage community as a completely non-invasive tool for the documentation and analysis of works of art [3]. Two different non-invasive reflectance spectroscopy techniques are currently employed for cultural heritage applications: Fiber Optics Reflectance Spectroscopy (FORS) and Imaging Spectroscopy (IS) [2]. The former uses fiber optics to convey light (typically exiting a monochromator) to the target object. Reflectance information is recovered in two possible ways: when a dual-beam approach is used, the incident light beam is split before being directed onto the object, and the unreflected beam is used as a reference to calculate the reflection coefficient. In the single-beam approach, the absolute reflected light intensity is measured. In this case, reflectance can be calculated after acquiring a reference white object. Dual-beam fiber optic spectrometers are very accurate but not easily portable. On the contrary, single-beam fiber optic spectrometers are more compact and easily transportable, but can lead to greater measurement errors.

FORS instrumentation operates in a point-wise fashion. On the contrary, IS determines spectral reflectance data for each pixel in a spatial image. Imaging spectrometers can be divided into two classes according to the way multispectral information is recovered. A first approach consists in putting a set of filters in front of the detector. The number of filters used in state-of-the-art solutions varies from 7 to 32, and the spectral resolution from 10nm (narrow-band filters) to 40nm (wide-band filters)[3]. Another approach consists in using a dispersive element to separate the different light components, which are then detected by a sensor (typically a CCD). In this case, higher spectral resolution ($<$1nm) can be achieved, but the received signal intensity is considerably lower than in the filter-based approach.

Imaging spectroscopy allows the recovery of the spectral reflectance of the whole target object (or parts of it). Therefore, not only a faithful color reproduction of the object can be achieved, but also more interesting tasks, such as the comparison of the spectral content of different parts of the object or image segmentation based on spectral features, can be performed. IS methods are generally less accurate than FORS ones, but allow a more exhaustive inspection of the spectral content of the target. It could be claimed that IS methods are sufficiently accurate if they allow the detection of significant spectral features in certain spots of an object, to which more accurate analysis can be restricted. In this logic, IS and FORS can be considered as complementary. The reliability of the spectral content analysis clearly depends on the accuracy of the spectral reflectance reconstruction, which in turn is determined by several factors, such as the instrument's spectral resolution, the measurement noise and the choice of the illumination source.

The aim of this study was to assess the performance of a spectral camera using a dispersive element imaging spectrograph to recover multispectral information. The instrument's nominal spectral sensitivity spans the visible and near-infrared (NIR) spectrum (400-1000nm). Our purpose is to use it to analyze the constituent materials and to attempt dating of a fragment of the mosaic of the St. Mark's Basilica in Venice. To do so, we need the recovered reflectance to be in good agreement with the true one, without distortion or spurious peaks. Not wishing to modificate the components of the camera (objective and CCD), we have mainly acted on the illumination, trying and possibly combining different sources.

This paper is organized as follows: Section 2 describes our spectral camera, Section 3 outlines the experimental trial, Section 4 explains how we evaluated the reconstruction performance and Section 5 describes the results. Section 6 draws the conclusions.

2. THE SPECTRAL CAMERA

A schematic drawing of the imaging spectrograph is shown in Fig. 1. The objective lens focuses the image of the target to be acquired on the plane of the input slit of the spectrograph. The light coming from a rectangular narrow strip conjugated with the slit enters into the spectrograph, is dis-

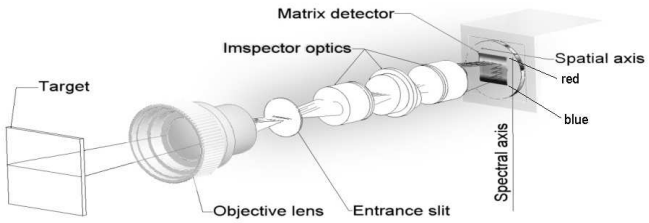

Figure 1: Shematic view of an imaging spetrograph [1].

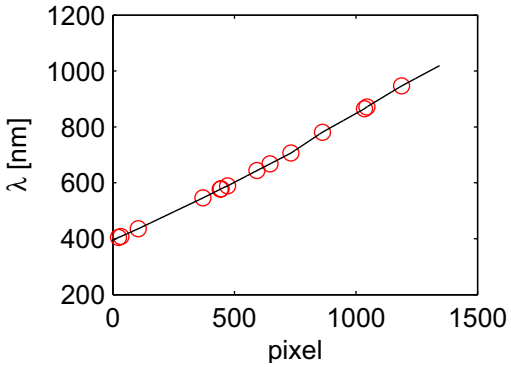

Figure 2: Spectral calibration curve.

persed by a dispersive element (prism or grating) and focused on the plane of the 2D detector. With reference to Fig. 1, the horizontal axis of the camera is the spatial axis, while the vertical axis is the spectral axis. The light coming from the same point on the target but with different wavelengths is focused on the sensor on the same column (i.e. the same spatial position) but in different rows (i.e. different spectral positions). A set of 2D spectral images is a series of monochromatic images of a 2D region on the target obtained by a scanning of the target in the direction perpendicular to the slit [4].

The choice of the objective focal length is imposed by the required field-of-view (FOV) in the direction parallel to the slit. Several objectives are currently available. For this study we used a Canon f=16mm, f/#1.4 objective, that matches the f/number of the spectrograph. The spectrograph is the Specim ImSpector V10 [1], which has a spectral window from 400 to 1000 nm. The entrance slit size is 9,8mm $\times$ 25μm. The sensor is the Hamamatsu C8484-05G. It is a progressive scan interline CCD with micro-lenses, 1024 (spatial) $\times$ 1344 (spectral) pixel format, 6.45μm $\times$ 6.45μm pixel size, 6.6mm $\times$ 8.7mm active area. The CCD is moderately cooled to reduce the thermal noise and increase the sensitivity. The camera has 10 e- rms readout noise, dynamic range of 1800:1 and quantum efficiency between 0.35 and 0.70 in the 400-750nm spectral interval. The FOV in the direction parallel to the slit is limited by the number of pixels in the spatial direction. Placing the instrument at 1 m from the target, a spatial sampling of 0.4mm can be obtained using the f=16mm objective. The scanning in the direction perpendicular to the slit is performed by a rotation of the spectrograph by means of a rotating stage (Physik Instrumente M-062).

2.1 Spectral calibration

The spectral calibration of an imaging spectrograph consists in determining the correspondence between pixel numbers and wavelengths. The calibration was performed by measuring the spectra of low pressure gas lamps which emit very narrow spectral lines characteristic of the gas in the lamp. The correspondence between pixels and wavelengths was found to be nearly linear (see Fig. 2). The spectral dispersion is 72.1 nm/mm and the spectral resolving element is 0.465 nm/pixel.

2.2 Reflectance measurement

Our imaging spectrograph measures absolute light intensities, therefore it is necessary to acquire a reference white signal under the same illumination conditions as the target object in order to calculate its spectral reflectance. In our experimental trial, the reference white signal was obtained by acquiring a Labsphere white tile with a flat 80% spectral reflectance over the interval 250-2500nm [5]. The reflectance of the target for any pixel $R_{m,n}$ was then calculated as:

$$R_{m,n} = 0.8 * \frac{S_{m,n} - D_{m,n}}{W_{m,n} - D_{m,n}}, \quad (1)$$

where $m = 1,\ldots,1024$ and $n = 1,\ldots,1344$ are the coordinates of the pixel within the sensor, $S_{m,n}$ is the acquired signal, $D_{m,n}$ is the dark signal of the camera and $W_{m,n}$ is the white signal. The subtraction of the dark signal accounts for the presence of the dark current signal in the CCD. The dark current signal is constant (apart from a random noise term) for a given temperature and exposure time. Therefore, it can be measured by acquiring a dark frame at the same exposure time and in the same temperature conditions as the actual frame [6].

Looking at eq. (1), it is clear that the spectral reflectance at a spatial point m on the target can be obtained as:

$$R_m = [R_{m,n}]_{n=1,\ldots,1344}, \quad (2)$$

with the corresponding wavelength array $\lambda = [\lambda_n]_{n=1,\ldots,1344}$ given by the spectral calibration procedure.

3. THE EXPERIMENTAL TRIAL

The light reflected by an object depends both on the object's surface reflectance characteristics and on the composition of the light illuminating the object. An ideal illumination source for the measurement of an object's spectral reflectance should thus exhibit a uniform spectrum over the whole desired wavelength range. Unfortunately, no existing illumination apparatus satisfies this condition over the visible and near-infrared spectrum, so that sub-optimal solutions must be adopted.

Moreover, other considerations concerning the spectral emission of a lamp should be taken into account. For example, when acquiring a painting or fresco, it is often unadvisable to use lamps with a strong emission in the infra-red spectrum as their heating may cause damages to the pictorial layer. As our spectral camera was primarily conceived for the acquisition of frescoed environments [7], we usually utilized lithium lamps due to their low emission both in the NIR and UV spectra. However, such precautions are not necessary when acquiring a mosaic, therefore we looked for other

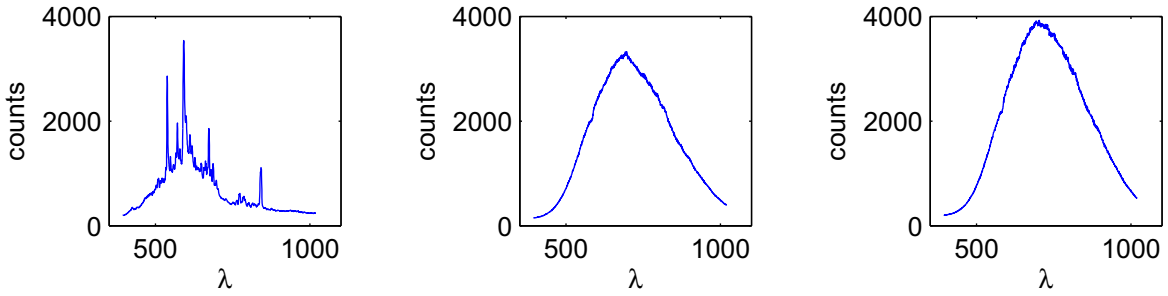

Figure 3: Spectrum of the lamps used in our study: (a) lithium lamp (b) halogen lamp (c) incandescence lamp.

kinds of lamps that would provide a sufficiently strong emission in the long-wavelength visible and NIR spectrum. Three different lamps were used in our experiments:

1. a Disano 250W Lithium lamp (with the spectrum shown in Fig. 3(a));
2. a Cixi Zhongfa Lamps 500W halogen lamp (Fig. 3(b));
3. an Osram 60W incandescence lamp (Fig. 3(c)).

It can be observed that the lithium lamp has strong emission in the blue-green region, while the halogen and incandescence lamps mainly emit in the red-NIR spectrum. However, it can easily be seen that the emission of all the lamps definitively drops around 850-900nm. Therefore, all reflectances were calculated in the 400-900nm interval.

Our experimental trial consisted in the acquisition of known reflectance objects under different illumination conditions. Four lamp configurations were used:

1. Lithium lamp alone. We chose this setup as it is the only one which may be extended to the acquisition of painted surfaces; as the lithium lamp has low emission in the red-NIR region, a correction function was derived for the measured spectral reflectances.
2. Lithium lamp *together with* halogen lamp. This setup has the advantage of combining the emissions of the two lamps without doubling the acquisition time.
3. Lithium lamp and halogen lamp in a sequence. The reflectance measurement was obtained by juxtaposing the spectral reflectance measured with the lithium lamp in the interval 400-600nm and that obtained with the halogen lamp in the 600-900nm interval.
4. Lithium lamp and incandescence lamp in a sequence, obtaining the spectral reflectance as in the previous case. The incandescence lamp was used instead of the halogen lamp because it has a slightly stronger emission in the NIR spectrum and because its spectrum looked smoother.

The acquired target was the Labsphere Pastel Color Standard set [5]. This set is made of eight highly diffusive tiles with colors spanning the visible spectrum. Their spectral reflectance is tabulated between 380nm and 830nm. No quantitative error evaluation was therefore possible in the 830-900nm interval.

For each target acquisition, five measurements were done to average down measurement noise. The camera exposure time was set so as to maximize the white signal dynamic without saturating the camera (saturation value is 4000 counts).

4. PERFORMANCE EVALUATION

A way of characterizing the accuracy of reflectance measurements could be that of calculating the CIELAB distances [8] between tabulated and measured reflectances. However useful this approach may be for colorimetry applications, it does not account for accuracy variations with wavelength. Therefore, we chose to characterize our system's performance by the error and the error standard deviation calculated as functions of wavelength and averaged over the tile set.

Remembering eq. (1) and eq. (2), we have that the mean reflectance for each tile can be calculated as:

$$\begin{aligned} R^i_m(\lambda) &= \frac{\frac{1}{5}\sum_{j=1}^5 S^{i,j}_m - \frac{1}{5}\sum_{j=1}^5 D^{i,j}_m}{\frac{1}{5}\sum_{j=1}^5 W^{i,j}_m - \frac{1}{5}\sum_{j=1}^5 D^{i,j}_m} = \\ &= \frac{\bar{S}^i_m - \bar{D}^i_m}{\bar{W}^i_m - \bar{D}^i_m} = \\ &= f(\bar{S}^i_m, \bar{W}^i_m, \bar{D}^i_m), \end{aligned} \tag{3}$$

where $i = 1,\ldots,8$ is the tile index and $j = 1,\ldots,5$ the acquisition index. From now on, we shall drop the pixel index m, with the understanding that we will consider the central pixel of each tile.

The reflectance error for each of the eight colors is therefore:

$$e^i(\lambda) = R^i(\lambda) - R^i_{tab}(\lambda), \tag{4}$$

where $R^i_{tab}(\lambda)$ is the tabulated spectrum of the i-th tile.

We now want to calculate the variance of the error from the variances of the experimentally observed variables $\{X^{i,j}\}_{j=1,\ldots,5}$, $X \in \{S,W,D\}$. The latter can be estimated as [9]:

$$\sigma^2_{X^i}(\lambda) = \frac{1}{4}\sum_{j=1}^5 (X^{i,j}(\lambda) - \bar{X}^i(\lambda))^2, \tag{5}$$

with the understanding that each observation is given by $X^{i,j}(\lambda) = \tilde{X}_i(\lambda) + w_j(\lambda)$, where $\tilde{X}_i(\lambda)$ is the "true" spectrum and $w_j(\lambda)$ the j-th realization of a random noise.

The variance of the derived variable $e^i(\lambda)$ can be calculated as (see [9]):

$$\sigma^2_{e^i} = \sum_{k=1}^3 \left(\frac{\partial f}{\partial \bar{X}^i_k}\right)^2 \sigma^2_{X^i_k} + 2\sum_{k=1}^3 \sum_{l=k+1}^3 \frac{\partial f}{\partial \bar{X}^i_k}\frac{\partial f}{\partial \bar{X}^i_l}\sigma_{X^i_k,X^i_l} + \sigma^2_{R_{tab}}, \tag{6}$$

where $X_1 = S$, $X_2 = W$, $X_3 = D$, $\sigma_{X_k^i,X_l^i}$ is the covariance between the variables X_k^i and X_l^i, $\sigma^2_{R_{tab}}$ the variance of the tabulated reflectance, and the dependence by λ has been omitted for the sake of clarity. As the variance of the tabulated reflectance is less than $2.5 \cdot 10^{-5}$ [5], it will be neglected in the following.

Looking at eq. (3), the partial derivatives can be easily calculated as:

$$\begin{aligned} \frac{\partial f}{\partial \bar{S}^i}(\lambda) &= \frac{1}{\bar{W}^i(\lambda) - \bar{D}^i(\lambda)}, \\ \frac{\partial f}{\partial \bar{W}^i}(\lambda) &= -\frac{\bar{S}^i(\lambda) - \bar{D}^i(\lambda)}{(\bar{W}^i(\lambda) - \bar{D}^i(\lambda))^2}, \\ \frac{\partial f}{\partial \bar{S}^i}(\lambda) &= \frac{\bar{S}^i(\lambda) - \bar{W}^i(\lambda)}{(\bar{W}^i(\lambda) - \bar{D}^i(\lambda))^2}. \end{aligned} \tag{7}$$

Lastly, the covariances $\sigma_{X_k^i,X_l^i}$ are given by:

$$\sigma_{X_k^i,X_l^i}(\lambda) = \frac{1}{4}\sum_{j=1}^{5}(X_k^{i,j}(\lambda) - \bar{X}_k^i)(X_k^{i,j}(\lambda) - \bar{X}_l^i). \tag{8}$$

Once we have obtained the error and error variance for each tile, we can average them over the eight tiles to obtain the average error (AE) and the average error variance as:

$$e(\lambda) = \frac{1}{8}\sum_{i=1}^{8} e^i(\lambda), \quad \sigma_e^2(\lambda) = \frac{1}{8}\sum_{i=1}^{8}\sigma^2_{e^i}(\lambda). \tag{9}$$

However, as the standard unit of uncertainty is standard deviation [9], we will eventually use the average error standard deviation (AESTD) instead of the variance. The AESTD is given by:

$$\sigma_e(\lambda) = \frac{1}{8}\sum_{i=1}^{8}\sigma_{e^i}(\lambda), \tag{10}$$

which is close to, but does not coincide with the square root of the variance expressed in eq. (9).

5. RESULTS

5.1 Lithium lamp

The AE and AESTD of the spectral reflectances acquired using the lithium lamp can be seen in Fig. 4(a). It can be noted that the AE greatly increases (in absolute value) after 750nm, in correspondence with the drop in the lamp emission. On the contrary, the AESTD increases (up to 8%[1]) between 400 and 420nm. The reason is that there are great differences in the reconstructed reflectances in the blue region. Namely, the measured reflectances for the red, yellow and orange tiles are zero over most of this interval. The reason is that in these cases three different phenomena combine: a drop in the lamp emission, a drop in the CCD sensitivity and a drop in the material reflectance. As a result, the measured reflected signal falls below the dark signal.

[1] In this case, percentage does not indicate a relative error, but is used in conformity with the corresponding notation for reflectance. However, it may also indicate the relative error with respect to the 100% white signal.

For the reasons stated in section 3, we tried to correct the measured spectra defining a mean correction function. To do so, we considered the ratio between measured and tabulated spectra, which should be one over the entire spectrum for perfectly reconstructed reflectances. We then defined a continuous piecewise linear function approximating the global reflectance behavior in a least-square sense, and used it to correct each reflectance. As can be seen in Fig. 4(b), there is indeed a global trend in the ratios, with the notable exception of violet in the red-NIR region. The AE and AESTD of the corrected reflectances can be seen in Fig. 4(c). It can be observed that, although slightly improved, the error still reaches -20% in the NIR region.

5.2 Lithium lamp in combination with halogen lamp

As can be seen in Fig. 5(a), the combined use of the lithium and halogen lamps brought an improvement in the red-NIR region, but also caused a decrease in the reconstruction performance in the blue region. The reason is that in order to use the two lamps simultaneously we had to halve the camera exposure time with respect to the previous case, so as to avoid camera saturation. This meant that in the spectral regions where just one of the two lamps had strong emission (the blue and red-NIR regions), we obtained an "average" performance between the two lamps, rather than the best of the two. This suggested using the two lamps in a sequence, instead of illuminating the target with both at the same time.

5.3 Lithium lamp and halogen lamp in a sequence

We recall that in this case the resulting spectral reflectance was obtained by juxtaposing the spectral reflectance measured with the lithium lamp between 400 and 600nm, and that acquired with the halogen lamp between 600 and 830nm. Looking at Fig. 5(b), one can see that the AE is indeed reduced to less than 5% in absolute value. However, confronting Fig.s 4(a) and 5(b), it can be observed that the lithium lamp outperforms the halogen lamp between 600 and 750nm. Rather than changing the juxtaposition threshold to a less intuitive value than the center of the considered spectrum, we decided to try another light source emitting in the red-NIR region.

5.4 Lithium lamp and incandescence lamp in a sequence

Using the incandescence lamp instead of the halogen lamp, the AE is reduced to less than 2% (in absolute value), with an AESTD of about 1% over the whole 420 - 830nm spectrum (for the 400-420nm interval the considerations done in subsection 5.1 still hold). Moreover, the AE is more uniform than in the previous case.

6. CONCLUSIONS

We assessed the performance of our spectral camera in the measurement of spectral reflectance in the 400-830nm interval by acquiring a set of colored calibrated tiles under different illumination conditions. We used a Lithium lamp, the Lithium lamp together with a halogen lamp, the Lithium and halogen lamps one after the other, and the Lithium and incandescence lamp in a sequence. In the last two cases, we obtained spectral reflectances as a juxtaposition of the reflectance measured with the Lithium lamp from 400 to 600nm and that acquired with the other lamp from 600 to

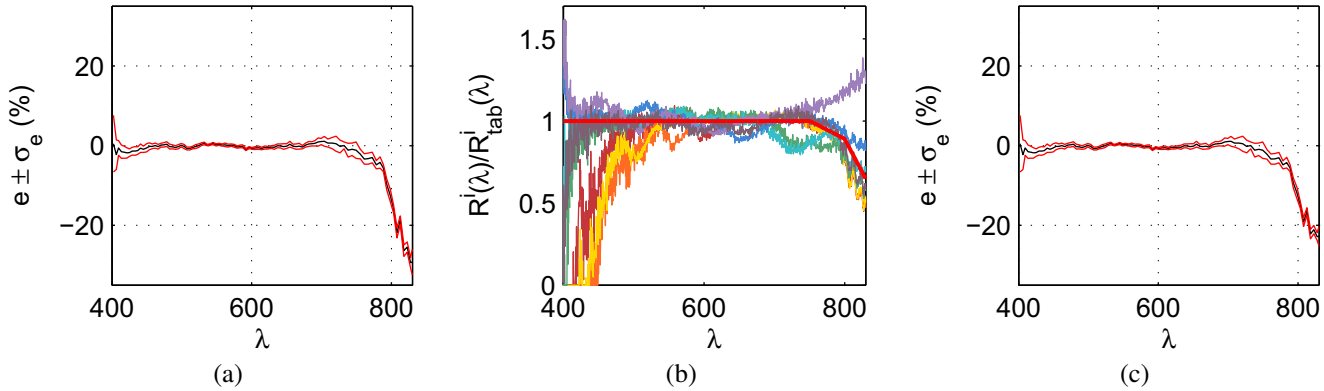

Figure 4: (a) average error (AE) and average error standard deviation (AESTD) with the lithium lamp (b) correction function for the spectra (c) AE and AESTD after the correction.

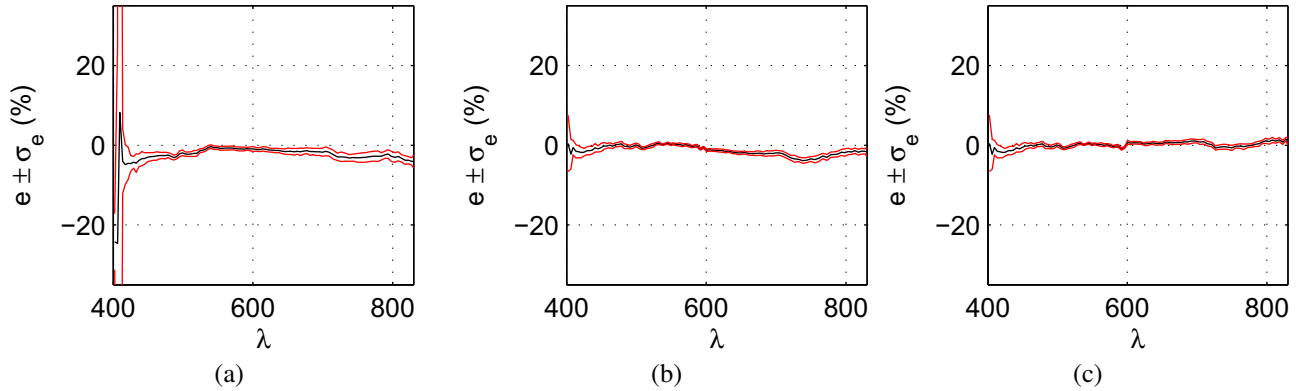

Figure 5: AE and AESTD with (a) the lithium lamp and the halogen lamp used together (b) the lithium lamp and the halogen lamp used in a sequence (c) the lithium lamp and the incandescence lamp used in a sequence.

830nm. To evaluate the system performance, we used the average error (AE) and the average error standard deviation (AESTD), calculated for each illumination setup and averaged over the eight-tile set. The best results were obtained with the Lithium and incandescence lamps used in a sequence. In this case, the absolute AE was less than 2% over the whole spectrum, and the AESTD less than 1% between 420 and 830nm and less than 8% between 400 and 420nm.

Acknowledgments

We would like to thank prof. Pietro Fiorentin and Elena Pedrotti of the Illuminating Engineering and Photometry Laboratory of the Department of Electrical Engineering of the University of Padova (Italy) for lending us the Labsphere Pastel Color Standard set and the 80% reflectance Labsphere white tile. We would also like to acknowledge Matteo Caldon, Carlo Tona and Filippo Ratti for their help in performing the acquisitions.

REFERENCES

[1] *www.specim.fi.*

[2] E. Ciliberto, G. Spoto, *Modern analytical methods in art and archeology*. John Wiley & sons, 2000.

[3] M. Barni, A. Pelagotti, A. Piva, "Image Processing for the Analysis and Conservation of Paintings: Opportunities and Challenges," *Signal Processing Magazine*, vol. 22, pp. 141–144, Sept. 2005.

[4] W.L. Wolfe, *Introduction to imaging spectrometers*. SPIE Tutorial Text Vol. 25, 1997.

[5] *www.labsphere.com*.

[6] S.B. Howell, *Handbook of CCD astronomy*. Cambridge University Press, 2006.

[7] N. Brusco, S. Capeleto, M. Fedel, A. Paviotti, L. Poletto, G. M. Cortelazzo, G. Tondello, "A system for 3D modeling frescoed historical buildings with multispectral texture information," *Machine Vision and Applications*, vol. 17, pp. 373–393, Dec. 2006.

[8] G. Wyszecki, W.S. Stiles, *Color science: concepts and methods, quantitative data and formulae*. John Wiley, 1982.

[9] ISO, *Guide to the Expression of Uncertainty in Measurement, GUM*.